RESOURCE/METHODOLOGY

Novel proteomic approach (PUNCH-P) reveals cell cycle-specific fluctuations in mRNA translation

Ranen Aviner,[1] Tamar Geiger,[2,3,4] and Orna Elroy-Stein[1,3,4]

[1]Department of Cell Research and Immunology, George S. Wise Faculty of Life Sciences, Tel Aviv University, Tel Aviv 69978, Israel; [2]Department of Human Molecular Genetics and Biochemistry, Sackler Faculty of Medicine, Tel Aviv University, Tel Aviv 69978, Israel

Monitoring protein synthesis is essential to our understanding of gene expression regulation, as protein abundance is thought to be predominantly controlled at the level of translation. Mass-spectrometric and RNA sequencing methods have been recently developed for investigating mRNA translation at a global level, but these still involve technical limitations and are not widely applicable. In this study, we describe a novel system-wide proteomic approach for direct monitoring of translation, termed puromycin-associated nascent chain proteomics (PUNCH-P), which is based on incorporation of biotinylated puromycin into newly synthesized proteins under cell-free conditions followed by streptavidin affinity purification and liquid chromatography-tandem mass spectrometry analysis. Using PUNCH-P, we measured cell cycle-specific fluctuations in synthesis for >5000 proteins in mammalian cells, identified proteins not previously implicated in cell cycle processes, and generated the first translational profile of a whole mouse brain. This simple and economical technique is broadly applicable to any cell type and tissue, enabling the identification and quantification of rapid proteome responses under various biological conditions.

[*Keywords*: cell cycle; proteomics; translation; protein synthesis; puromycin; PUNCH-P]

Supplemental material is available for this article.

Received April 3, 2013; revised version accepted July 15, 2013.

mRNA translation is a key step in gene expression that attracts increasing attention at the systems biology level. In past decades, major efforts were invested in studying transcription regulation, while research focusing on post-transcriptional control has lagged behind. Although mRNA levels are commonly used as a proxy of protein amounts, comparative genomic and proteomic analyses of different species and cell types have shown that mRNA and protein levels do not correlate perfectly, thereby stressing the important contribution of translation control and protein stability to gene expression (Vogel and Marcotte 2012). This provides cells with the plasticity needed to rapidly modulate gene expression in response to changes in environmental conditions (e.g., cellular stress) and also for fine-tuning of protein levels during cell cycle progression, proliferation, and differentiation (Calkhoven et al. 2002; Holcik and Sonenberg 2005). The ability to identify and quantify the proteins produced in a population of cells under various conditions is therefore essential to our understanding of the processes underlying gene expression.

Traditionally, translation rates have been monitored by metabolic labeling of cells with radioactive amino acids. For high-resolution identification and quantification of proteins, metabolic labeling was combined with mass spectrometric (MS) analysis, and the radioactive amino acids were replaced by stable isotope-labeled (SILAC [stable isotope labeling by amino acids in cell culture]) amino acids. To distinguish newly synthesized from pre-existing proteins, cells are pulse-labeled with SILAC amino acids, allowing only proteins produced during the pulse to incorporate the label. This method, termed pulsed SILAC (pSILAC), is successfully used to detect long-lasting changes in protein production and degradation but is incompatible for studying rapid fluctuations because accurate quantification of SILAC pairs requires relatively long pulses (Schwanhausser et al. 2009).

[3]These authors contributed equally to this work.
[4]Corresponding authors
E-mail ornaes@tauex.tau.ac.il
E-mail geiger@post.tau.ac.il
Article published online ahead of print. Article and publication date are online at http://www.genesdev.org/cgi/doi/10.1101/gad.219105.113.

Another proteomic approach is based on incorporation of a modified methionine analog called azidohomoalanine (AHA), which is subsequently derivatized to tagged reporter molecules or an affinity purification matrix through click chemistry. This method has been successfully used to visualize mRNA translation in situ; however, it requires predepletion of intracellular endogenous methionine followed by supplementation of the amino acid analog, both of which can result in cellular stress and potential alteration of translation patterns (Vaughan et al. 1971; Kramer et al. 2009). AHA incorporation into tRNA was also shown to occur more slowly than methionine, possibly introducing a measurement bias (Kiick et al. 2002). Attempts to use AHA labeling for MS identification of newly synthesized proteins either alone or in combination with SILAC have shown that this approach is limited to detection of up to several hundreds of proteins (Dieterich et al. 2006; Eichelbaum et al. 2012; Howden et al. 2013).

Protein synthesis has also been indirectly monitored by deep sequencing of ribosome-protected mRNA fragments using a technique called ribosome profiling, otherwise known as ribosome footprinting or ribo-seq (Ingolia et al. 2009). This method involves nuclease digestion of cell extracts to degrade all mRNA molecules that are not protected by ribosomes, leaving out short undigested RNA fragments. These are isolated by a series of purification steps, including PAGE fragment size selection and rRNA subtractive hybridization, followed by sequencing. Ribo-seq is a powerful technique for investigating translation at a subcodon resolution, measuring translation efficiency, and mapping novel ORFs (Guo et al. 2010; Lee et al. 2012). In addition, it does not require in vivo labeling that may induce stress. However, a limitation of ribo-seq is that it only generates a prediction of protein synthesis based on the steady-state amounts of ribosome-bound mRNA molecules. This may be misleading in some cases, as inhibition of protein synthesis is not always accompanied by a decrease in the number of ribosomes associated with the encoding mRNA (Clark et al. 2000; Nottrott et al. 2006; Petersen et al. 2006; Sivan et al. 2007).

In another alternative approach, the naturally occurring antibiotic puromycin is used to label and detect newly synthesized proteins. Puromycin, a tyrosine-tRNA mimetic, is catalytically incorporated by the ribosome into the C terminus of elongating nascent polypeptide chains in a sequence-independent manner. Incorporation leads to translation termination and release of C-terminally truncated peptides bearing a puromycin moiety (Pestka 1971). This so-called "puromycylation" reaction has so far been studied by immunoblotting, immunofluorescence, and flow cytometry using puromycin-specific antibodies and fluorescent or biotinylated puromycin derivatives (Starck et al. 2004; Schmidt et al. 2009; David et al. 2012). In cultured cells, puromycylation followed by Western blotting with an anti-puromycin antibody is used to monitor translation rates in place of radioactive metabolic labeling (Schmidt et al. 2009). Puromycin and its derivatives also enabled in situ visualization of protein synthesis (David et al. 2012; Liu et al. 2012) and isolation of a specific protein produced in rabbit reticulocyte lysate (Starck et al. 2004). However, to the best of our knowledge, attempts to use these antibodies for immunoprecipitation have been unsuccessful.

In this study, we describe a method that combines biotinylated puromycin with MS analysis to globally label newly synthesized proteins and monitor mRNA translation. The method involves isolation of ribosomes by ultracentrifugation followed by cell-free labeling of nascent polypeptide chains with 5′ biotin-dC-puromycin 3′ (Biot-PU), capture on immobilized streptavidin, and analysis by liquid chromatography-tandem MS (LC-MS/MS) (Fig. 1). This work flow leads to the identification of thousands of newly synthesized proteins, generating a snapshot of the cellular translatome. We used this method, termed puromycin-associated nascent chain proteomics (PUNCH-P), to study global cell cycle-dependent variations in translation and identify proteins that are differentially synthesized at specific stages.

Results

Labeling, capture, and MS analysis of newly synthesized proteins from mammalian cells

The development of a method for proteomic analysis of newly synthesized proteins involved multiple steps of

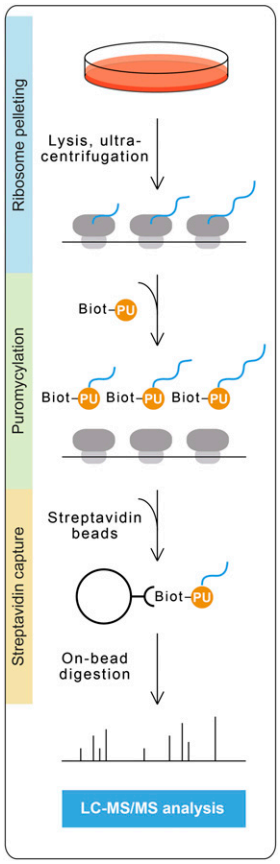

Figure 1. Experimental setup of PUNCH-P. Ribosomes are extracted from cultured cells by ultracentrifugation on a sucrose cushion. Ribosomes are then incubated with the labeling reagent Biot-PU, and labeled newly synthesized proteins are isolated by streptavidin affinity purification and analyzed by LC-MS/MS.

calibration and optimization. As puromycylation can be performed in either cultured cells or isolated polysomes (Blobel and Sabatini 1971; David et al. 2012), we first sought to compare the incorporation of puromycin and Biot-PU under these two experimental conditions. To this end, cultured HeLa cells or polysomes that were isolated by ultracentrifugation on a sucrose cushion were treated with either 1 μM puromycin or 1 μM Biot-PU for 30 min at 37°C. Equal amounts of total protein were resolved on an SDS-PAGE, and the membrane was probed sequentially with a commercial anti-puromycin antibody and a streptavidin-HRP conjugate to detect proteins bearing a terminal puromycin or Biot-PU, respectively. Underivatized puromycin efficiently labeled newly synthesized proteins in both intact cultured cells and isolated polysomes (Supplemental Fig. S1). In contrast, Biot-PU incorporation was only detected in isolated polysomes, possibly due to reduced permeability through the plasma membrane. We reasoned that cell-free puromycylation of isolated polysomes may in fact be preferable, as it does not affect the pattern of protein synthesis or depend on the duration of labeling for obtaining sufficient amounts of puromycylated proteins to allow MS detection. Without a pulse time limitation, Biot-PU can be used to study changes in mRNA translation that occur very rapidly. Furthermore, extraction of ribosomes prior to puromycylation depletes the reaction mixture of endogenously biotinylated proteins that otherwise compete for streptavidin binding and may significantly affect the signal to noise ratio (Robinson et al. 1983; de Boer et al. 2003).

To determine the amount of Biot-PU required for complete labeling of nascent polypeptide chains, we incubated a fixed amount of ribosomes with increasing amounts of Biot-PU (Supplemental Fig. S2). A ratio of 1 pmol of Biot-PU to 1 OD_{254} ribosomes provided complete labeling and was therefore maintained in all future experiments. We then analyzed the time course of Biot-PU incorporation and found that it proceeds rapidly and reaches saturation within 15 min (Fig. 2A). Incubation on ice or addition of cycloheximide, a competitive inhibitor of the puromycin reaction (Hobden and Cundliffe 1978), each reduced signal intensity, confirming the involvement of ribosome catalysis in the incorporation of Biot-PU (Fig. 2B).

Pretreatment with cycloheximide is commonly used to arrest elongating ribosomes prior to lysis and fractionation to prevent ribosome runoff during harvesting or ultracentrifugation. To examine whether omitting cycloheximide has a destabilizing effect on ribosomes in our experiments, we compared HeLa cells harvested with or without pretreatment with 100 μg/mL cycloheximide for 5 min and fractionated on a linear 10%–50% sucrose gradient. The data showed that omitting cycloheximide from the harvesting, lysis, and sucrose fractionation steps has a very minor destabilizing effect on polysome size (Supplemental Fig. S3).

To confirm that puromycin labeling correlates with the presence of nascent polypeptide chains, we monitored the cosedimentation of puromycylated peptides with ribosomes by fractionating a saturated Biot-PU-labeling reaction on a similar sucrose gradient under low-salt conditions that prevent ribosome dissociation (Fig. 2C, top panel; Blobel and Sabatini 1971). Western blot analysis of gradient fractions corresponding to the entire range of monosomes through heavy polysomes showed that both the mean molecular weight and the intensity of puromycylated peptides increase with polysome size (Fig. 2C, bottom panel, densitometry). This distribution is consistent with nascent polypeptide chains because heavy faster-sedimenting polysomes translate mRNAs with longer ORFs and produce larger amounts of protein in total.

To examine the applicability of the method to additional cell lines, we isolated ribosomes from HEK293

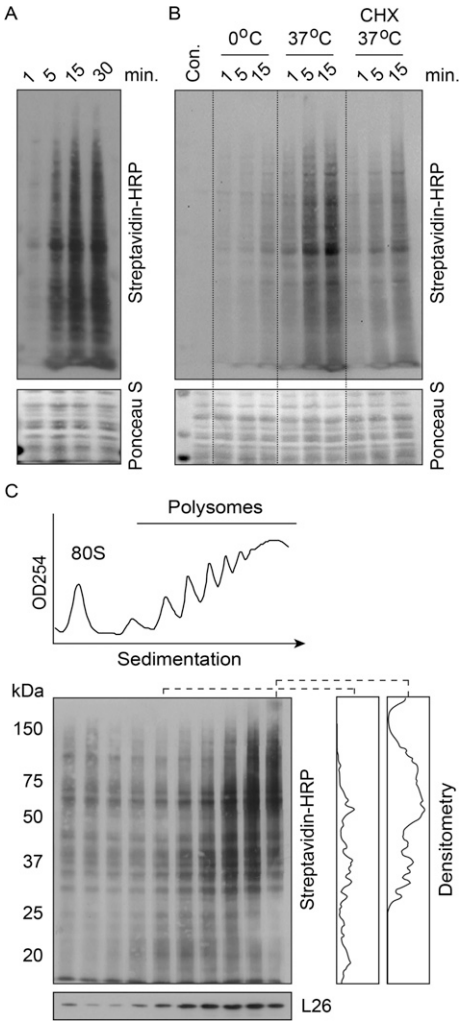

Figure 2. Biochemical characterization of PUNCH-P. (*A*,*B*) Newly synthesized proteins were labeled by Biot-PU for the indicated times and under the indicated conditions and detected by Western blotting using streptavidin-HRP. (*C*) Newly synthesized proteins labeled by Biot-PU were fractionated on a linear 10%–50% sucrose gradient, and fractions corresponding to the entire range of monosomes to heavy polysomes were collected and probed by Western blotting. (*Top* panel) rRNA absorption at 254 nm, showing the positions of 80S monosome and polysomes. (*Bottom* panel) Western blotting of gradient fractions using streptavidin-HRP or anti-ribosomal protein L26 antibody. Vertical line traces on the *right* represent the densitometry of lane *5* (light polysomes) and lane *10* (heavy polysomes).

and RAW264.7 cells and analyzed nascent chain puromycylation as above. Western blot analysis showed that the labeling reaction proceeds efficiently in these cell types, revealing a different repertoire of labeled proteins (Supplemental Fig. S4).

The use of Biot-PU instead of puromycin allowed us to harness the extraordinary affinity between biotin and streptavidin to increase binding specificity and eliminate strong background binders; e.g., ribosomal proteins. We adopted a procedure that consists of overnight incubation with streptavidin beads under stringent denaturing conditions (2% SDS, 8 M urea) and extensive washes prior to elution (Tagwerker et al. 2006). This procedure resulted in very low background binding as compared with the manufacturer's recommended low-stringency protocol while retaining the same levels of the puromycylated peptides (Supplemental Fig. S5).

Using this procedure, we set out to identify and quantify newly synthesized proteins in cycling HeLa cells. Western blotting confirmed that nascent peptides were labeled and captured with high specificity and that components of the translation machinery were removed, as evidenced by the absence of ribosomal protein L26 from the streptavidin eluate (Fig. 3A). Streptavidin beads from similar amounts of puromycylation and control reactions were then subjected to on-bead trypsin digestion followed by single LC-MS/MS runs on the Q-Exactive MS. Data were analyzed with MaxQuant software, and a Student's *t*-test was used to compare triplicates of puromyclated proteins and control samples. Of 3244 proteins identified in at least two replicates, 3072 were specific to the puromycylated samples relative to nonpuromycylated controls (false discovery rate [FDR] = 0.05, S0 = 0.5) (Fig. 3B; Supplemental Table 1), representing newly synthesized proteins. The technical reproducibility of this experiment was high, with an average Pearson correlation of 0.96 between replicates (Fig. 3C).

To determine whether polysome isolation and labeling procedures influence the identity or relative quantity of the proteins detected, we performed a PUNCH-P analysis of cycling HeLa cells pretreated with emetine, a highly effective irreversible inhibitor of translation elongation that does not interfere with puromycylation (David et al. 2012). We reasoned that any bias introduced by the isolation procedure itself should be eliminated in the presence of emetine, which blocks translation in vivo prior to harvesting and therefore protects from downstream in vitro effects. PUNCH-P profiles for emetine-treated and control cells were strikingly similar in both coverage and relative quantity of proteins detected (r = 0.98), suggesting that no bias is introduced during the in vitro sample preparation procedure (Supplemental Fig. S6; Supplemental Table 1).

Comparative analysis of protein synthesis using PUNCH-P, ribo-seq, and pSILAC

To further evaluate and validate PUNCH-P, we compared it with pSILAC and ribo-seq, two established methods that are used for studying translation at the protein and mRNA levels, respectively. A principle difference between these methods is that PUNCH-P and ribo-seq generate an in vitro snapshot of translation, while pSILAC is based on the in vivo accumulation of labeled proteins during the translation process. In light of these differences, we first compared two pulse durations of pSILAC to determine whether a minimum pulse of 2 h allows reproducible quantification of newly synthesized proteins, as previously reported (Schwanhausser et al. 2009; Eichelbaum et al. 2012). To this end, we pulse-labeled cycling HeLa cells for 2 or 10 h with either heavy or medium-heavy stable isotope amino acids, thereby generating duplicate analyses in single MS runs. While the 10-h pulse yielded reproducible results with a high correlation between heavy and medium-heavy peptides in the same run and a narrow distribution of heavy/medium-heavy ratios between separate runs (r_{avg} = 0.93, median absolute deviation [MAD] of 0.12–0.15), the 2-h pulse showed poor reproducibility (r_{avg} = 0.75, MAD 0.54–0.56) due to insufficient labeling and very large SILAC ratios (Supplemental Fig. S7; Supplemental Table 2). We therefore used the 10-h pSILAC measurements for further comparisons.

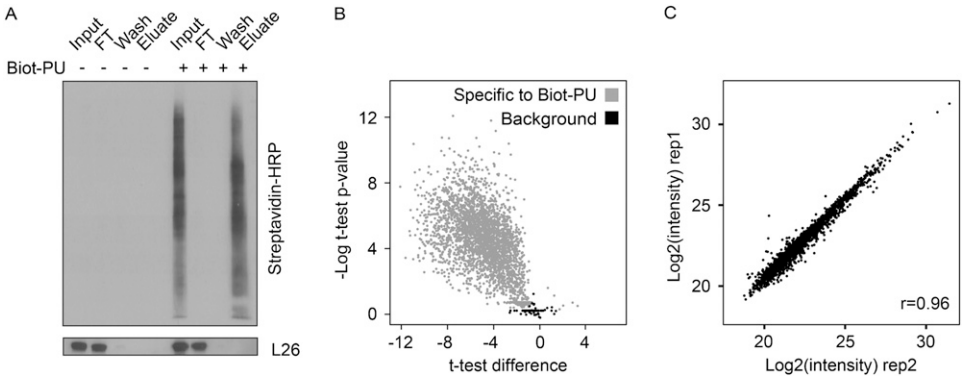

Figure 3. PUNCH-P analysis of cycling HeLa cells. (*A*) Puromycylation and control samples were incubated with streptavidin beads under stringent conditions, and puromycylated newly synthesized proteins were eluted following extensive washing. Equal volumes of starting material (input), flowthrough (FT), wash, and eluate were analyzed by Western blotting. Ribosomal protein L26 is shown as control for removal of ribosomes from the eluate. (*B*) Volcano plot of proteins identified by MS in puromycylated compared with control samples. (*C*) Scatter plot showing the high technical reproducibility of PUNCH-P.

Based on observations that steady-state protein levels in mammalian cells are best explained by translation rates (Schwanhausser et al. 2011), we expected the results of each of the above methods to correlate well with overall protein abundance. Therefore, we compared PUNCH-P, 10-h pSILAC, and ribo-seq results (Guo et al. 2010) with publically available whole-proteome analysis of cycling HeLa cells (Nagaraj et al. 2011) and found that the correlation was similar for all three methods (r = 0.41, 0.40, and 0.42, respectively). This suggests that the methods are similarly accurate in quantifying translation products. However, the correlation between PUNCH-P and 10-h pSILAC (r_{avg} = 0.60) was significantly higher than the correlation between ribo-seq and either PUNCH-P or pSILAC (r_{avg} = 0.37 and r_{avg} = 0.43, respectively) (Fig. 4A,B), possibly due to technical differences in detection between MS and deep-sequencing techniques.

In terms of coverage, PUNCH-P identified and quantified thousands of proteins per sample—more than 10-h pSILAC (3072 and 2143, respectively, both analyzed by single 4-h LC-MS/MS runs) but less than ribo-seq (6238 transcripts, sequenced in two lanes per sample). Because ribo-seq coverage depends on the number of lanes used to sequence a single sample, the cost of analysis increases proportionally to the desired depth. PUNCH-P coverage, on the other hand, depends on the amount of starting material (as discussed below) and can also be increased by standard proteomic approaches, including peptide prefractionation and longer overall MS measurement time per sample.

Cell cycle-specific fluctuations in mRNA translation

After establishing that PUNCH-P performs well compared with current alternatives, we applied it to study changes in translation throughout the cell cycle as a test case. Such analysis cannot be accomplished by pSILAC due to the short duration of specific cell cycle phases (e.g., mitosis, which lasts 40–90 min in HeLa cells) (Rao and Engelberg 1968; Sigoillot et al. 2011); it is also challenging for ribo-seq because of the high costs associated with deep-sequencing analysis of a large number of samples.

For cell cycle synchronization, we used double-thymidine block to arrest cultured cells at the G1/S boundary and then released them in fresh medium to allow synchronous progression (Sivan et al. 2011). While the efficiency of synchronization under these conditions is not maximal, it eliminates the necessity of using drugs that arrest progression by inhibiting DNA replication (e.g., mimosine) or microtubule polymerization (e.g., nocodazole) and may confound the results due to nonphysiological effects on translation. We showed previously that arresting cells in mitosis using nocodazole leads to disassembly of polysomes, while a similar effect is not observed in thymidine-synchronized mitotic cells (Sivan et al. 2011).

To generate a global profile of protein synthesis throughout the cell cycle, we harvested thymidine-synchronized HeLa cells at four time points, corresponding to peak S phase, G2/M boundary, mitotic exit, and peak G1 phase, based on fluorescent analysis of DNA content (Fig. 5, bottom). Synchronization was performed in triplicates,

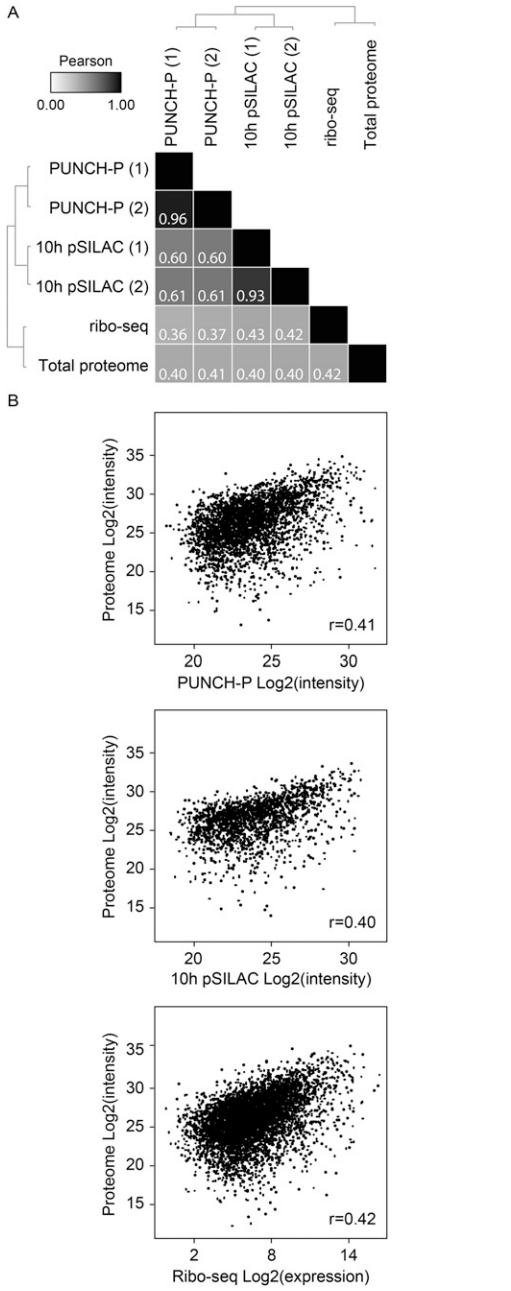

Figure 4. Comparison of PUNCH-P, 10-h pSILAC, and ribo-seq. (*A*) Heat map showing Pearson correlation between the methods for measuring protein synthesis and HeLa whole-cell proteome. (*B*) Representative scatter plots show the correlation between HeLa whole-cell proteome and PUNCH-P, 10-h pSILAC, and ribo-seq.

and the samples were processed in parallel for PUNCH-P analysis. A total of 5105 proteins were identified in at least two of three samples, of which 4984 were specific to the puromycylated samples relative to nonpuromycylated controls. ANOVA analysis of the differences between cell cycle stages revealed that, while the majority of proteins (4653, or ~93%) are synthesized at similar levels throughout the cell cycle, a subclass of 339 proteins shows statis-

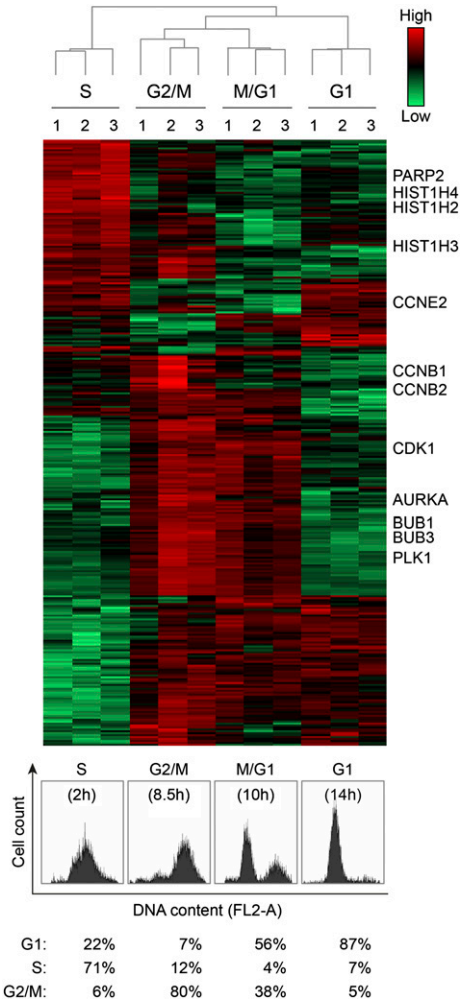

Figure 5. Cell cycle-related dynamics in protein synthesis. Hierarchical clustering of proteins was performed on logarithmized intensities after *Z*-score normalization of the data. The heat map shows proteins with statistically significant differences in synthesis throughout the cell cycle. Selected proteins from each cluster are indicated on the *right*. Flow cytometry analysis of DNA content using propidium iodide is shown in the *bottom* panel. Respective cell cycle stages are indicated, with time after release from second thymidine block in parenthesis and percentage of cells in each phase shown *below*.

tically significant variation (FDR = 0.05), representing a unique signature of cell cycle-specific protein expression (Supplemental Table 4). Hierarchical clustering of these fluctuating proteins shows clear segregation into several distinct protein clusters (Fig. 5), which highlight subclasses of functionally interconnected proteins that may play important roles in cell cycle progression. The largest cluster, consisting of proteins that are highly translated during mitosis, includes pivotal mitotic regulators; e.g., CCNB1/2 (cyclin B1/B2) and CDK1 (cyclin-dependent kinase 1). The cluster of proteins highly translated during S phase includes histones and proteins involved in DNA replication and repair. Interestingly, the synthesis of some S-phase proteins is already induced at G1; this cluster includes CCNE2 (G1/S-specific cyclin E2), a classical marker of G1/S transition, as well as several components required for DNA replication (see the Discussion).

To validate some of these results and provide further evidence for the potential of PUNCH-P to measure differences in translation of specific mRNAs, we analyzed the polysome association of selected mRNAs in S and M phase. We chose two proteins whose PUNCH-P expression remained stable throughout the cell cycle and six proteins whose expression fluctuated between S and M phase. Such fluctuations at the protein level can result from differences in total mRNA abundance, translation efficiency, or both. We initially compared the polysome profiles of HeLa cells synchronized to S and M phase and found no differences in polysome size (Fig. 6A, top panel). Next, we extracted total RNA from each of seven polysomal fractions ranging from light to heavy polysomes (Fig. 6A, bottom panel) and measured the abundance of specific mRNAs in each fraction using SYBR fast quantitative PCR (qPCR). As predicted, we found that the relative amount and polysomal distribution of the two transcripts encoding for nonfluctuating proteins (calreticulin [CALR] and cytochrome C [CYCS]) remained constant between the different cell cycle stages (Fig. 6B,C). We then measured the amount of the six transcripts encoding for fluctuating proteins in each polysomal fraction and normalized the results to *CALR* mRNA to allow a more accurate quantitative comparison of mRNA amounts in the different gradients. As predicted by PUNCH-P, the amounts of polysome-associated *FOSL1* (FOS-like antigen 1), *CCRN4L* (also called nocturnin), and *BRIP1* (Fanconi anemia group J protein 1) were significantly higher in S phase (Fig. 6D). Similarly, the amounts of polysome-associated *CCNB1* (cyclin B1), *GPSM2* (G-protein signaling modulator 2), and *PCF11* (pre-mRNA cleavage complex 2 protein) mRNA were higher in M phase, consistent with PUNCH-P results (Fig. 6E). In addition to the differences in absolute amounts, we calculated relative mRNA distribution between heavy (five or more) and light (less than five) polysomes as a percentage of total polysomes. While some mRNAs showed little difference in relative distribution, others changed considerably. Association of *CCRN4L* and *BRIP1* mRNAs with heavy polysomes decreased from 82.4% and 43.3% in S phase to 73.5% and 29.2% in M phase, respectively. Similarly, association of *CCNB1* mRNA with heavy polysomes increased from 63.80% in S phase to 84.30% in M phase, as expected for an mRNA that is translationally up-regulated during mitosis (Groisman et al. 2000).

Generating a whole mouse brain translatome

A unique advantage of this method, which analyzes translation based on ex vivo labeling, is its applicability to tissue samples, where in vivo labeling is highly challenging. As a test case, we chose to analyze the translatome of a developing mouse brain. Ribosomes were isolated from brains of three 3-wk-old C57BL mice followed by Biot-PU incorporation. Western blotting confirmed efficient label-

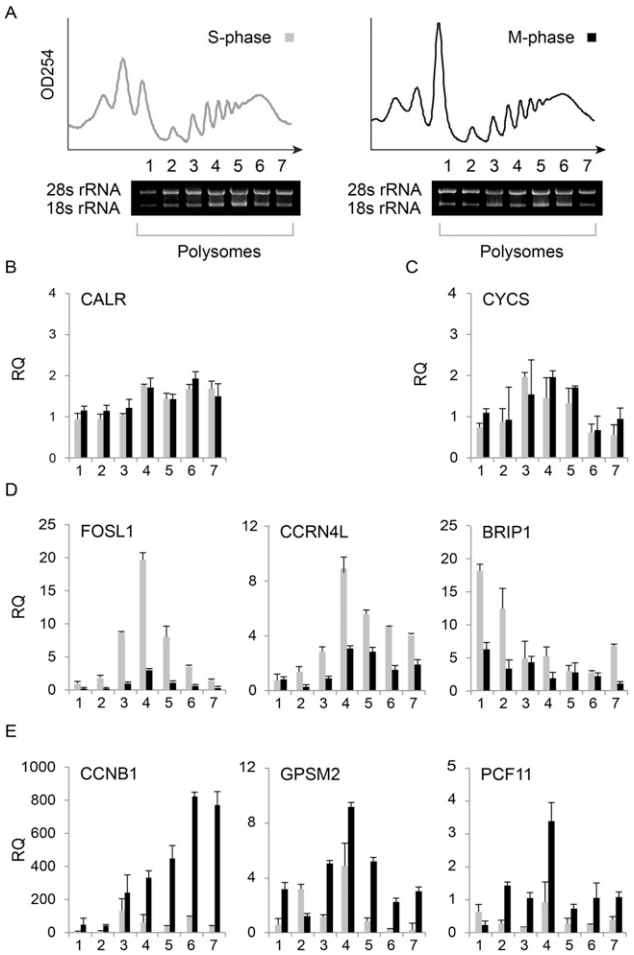

Figure 6. qPCR validation of PUNCH-P results. (*A*, *top* panel) Polysome profiles of HeLa cells synchronized to S and M phase by double-thymidine block. (*Bottom* panel) Total RNA extracted from each of the polysomal fractions visualized by ethidium bromide staining. (*B*,*C*) Polysomal association of nonfluctuating mRNAs encoding for CALR (*B*) and CYCS (*C*). (*D*) Polysomal association of mRNAs encoding for proteins that were elevated in S phase according to PUNCH-P. (*E*) Polysomal association of mRNAs encoding for proteins that were elevated in M phase according to PUNCH-P. Graphs show mean ± SD of qPCR replicates for one of three independent experiments with similar results. *C*–*E* represent qPCR results normalized to CALR.

ing of nascent polypeptide chains (Supplemental Fig. S8A). Streptavidin affinity purification and on-bead digestion followed by LC-MS/MS analysis identified just over 400 proteins specific to the puromycylated samples. This number was increased fivefold (to 2187) when three brain samples were pooled and analyzed together, confirming that starting material is an important determinant of proteome coverage in PUNCH-P analysis (Supplemental Fig. S8B; Supplemental Table 5).

Discussion

In this study, we describe the development of a novel proteomic approach for monitoring translation based on direct measurement of protein amounts without pulse duration limitations. We show that PUNCH-P is equally correlative to steady-state protein levels as pSILAC and ribo-seq, suggesting that it quantitatively detects actively synthesized proteins. Unlike pSILAC, PUNCH-P does not have a minimum pulse time requirement and can therefore be used to detect rapid changes in protein synthesis without influence from protein degradation. While PUNCH-P cannot compete with the single-nucleotide resolution of ribo-seq, it involves simple and rapid experimental setup and data analysis, with turnaround times of ~2 d from sample preparation to analyzed data. It is also economical, at ~1% of the cost of ribo-seq, and therefore suitable for the analysis of larger sets of samples. As such, it can also be used to supplement or validate ribo-seq results on a larger scale.

Employing these unique strengths of PUNCH-P, we generated the first atlas of cell cycle-dependent translation. Progression in the cell cycle is known to depend on complex interactions and feedback loops that are based on the temporally precise accumulation and activation of regulatory proteins; e.g., cyclins and CDKs (Lindqvist et al. 2009). While degradation and post-translational modifications have long been implicated in the regulation of cell cycle progression, the relative contribution of translation has yet to be quantified at a global level. Not surprisingly, our results suggest that differential translation may also play an important part in this regulation. We show that synthesis of functionally related proteins is coordinated through the cell cycle and identify novel proteins not previously implicated in cell cycle processes that can serve as a starting point for future research.

The network of proteins with increased synthesis during M phase reveals that mRNA translation is significantly involved in the mitotic program, perhaps more so than other stages of the cell cycle (Supplemental Fig. S9). Key proteins whose synthesis is elevated during M phase include pivotal mitotic regulators; e.g., CCNB1/2 (cyclin B1/B2) and CDK1; PLK1, NEK2, and AURKA kinases, which are involved in functional centrosome maturation and spindle stability; CDC20, which activates the anaphase-promoting complex (APC); and BUB1, which phosphorylates CDC20 as part of mitotic checkpoint complex (MCC) to prevent premature anaphase (highlighted in Supplemental Fig. S9A). Interestingly, of the 10 members of the kinesin motor protein superfamily found to be elevated in M phase, only some have a known role in mitosis (e.g., KIF20B and KIF23) (Miki et al. 2001). Identification of new kinesins that play a part during mitosis or upon entry to G1 may be of clinical significance, as mitotic kinesins are considered potential targets for anti-cancer interventions (Huszar et al. 2009).

PUNCH-P detected increased synthesis of histones in S phase (Supplemental Fig. S9B), consistent with the known temporal relationship between histone expression and DNA synthesis (Marzluff and Duronio 2002). Histone mRNA translation is regulated in part by a conserved stem–loop structure that recruits SLBP (stem–loop-bind-

ing protein), which is synthesized in late G1 and degraded upon exit from S phase (Whitfield et al. 2000). Indeed, although SLBP is most abundant in S phase, PUNCH-P identified increased SLBP synthesis in G1 (Supplemental Table 4). The transcription factors ATF3 and NFKB1/B2, which play a role in the intra-S-phase checkpoint and can be induced by DNA damage (Joyce et al. 2001; Fan et al. 2002), are also found in our S-phase list, as well as PARP2 (Supplemental Fig. S9B), which was recently reported to possess transcriptional repression activity by recruiting histone deacetylases and methytransferase to the promoter of cell cycle-related genes (Liang et al. 2013).

Proteins with increased synthesis in both G1 and S include regulators of G1/S transition; e.g., CCNE2, which is known to reach peak nuclear abundance in late G1 (Mumberg et al. 1997). In keeping with this observation, it is tempting to speculate that proteins such as ORC3 (origin recognition complex subunit 3) and DSN1 (kinetochore-associated protein), both enriched in our G1- and S-phase lists, are synthesized late in G1 to allow timely DNA synthesis and recognition of sister chromatids following replication. Interestingly, SMC1A (structural maintenance of chromosomes protein 1A), a protein required for sister chromatid cohesion (Losada and Hirano 2005) was detected by PUNCH-P in S phase, suggesting that its synthesis peaks during DNA replication, consistent with a possible role in DNA repair (Kim et al. 2002).

Of the proteins chosen for mRNA validation (Fig. 6), some have known roles that relate to either S or M phase, while others are implicated as such by the present study. FOSL1 is required for initiation of DNA synthesis (Riabowol et al. 1992), GPSM2 is important for spindle pole orientation (Yasumi et al. 2005), and CCNB1 is a major mitotic regulator whose protein levels peak during G2/M (Pines and Hunter 1989). In contrast, CCRN4L is a circadian deadenylase that turns off the expression of genes in a rhythmic fashion (Garbarino-Pico and Green 2007) but has no known role in the cell cycle; our work shows that CCRN4L is translationally up-regulated and may therefore play a part in S phase. Furthermore, PCF11 has not been implicated in cell cycle-related processes but was shown to interact with Rhn1, which is required for suppression of meiotic mRNAs in mitotically dividing fission yeast (Sugiyama et al. 2012), suggesting a role for PCF11 in mitosis. Additional research is needed to better characterize the involvement of CCRN4L and PCF11 in S and M phase, respectively.

An exciting prospect of PUNCH-P is its unique ability to monitor mRNA translation in whole tissues, which is challenging with ribo-seq and nearly impossible with pSILAC. While tissues with lower translation activity may require pooling to achieve efficient PUNCH-P detection, the test case reported here of a mouse brain analysis confirms that PUNCH-P is indeed applicable to tissues. Based on these results, we estimate that PUNCH-P can be used with any cell type or tissue and may thus represent an important technological advance in studying rapid proteome responses to stress, stimulus, or pharmacological perturbation at a tissue-specific level.

Materials and methods

Reagents and antibodies

Biot-PU was custom-synthesized by Dharmacon according to Starck et al. (2004). Streptavidin agarose beads were from Pierce Biotechnology. HRP-conjugated streptavidin for Western blotting was from R&D Systems or Vector Laboratories (Vectastain Elite ABC). Anti-puromycin antibody (12D10) was from Millipore. Control antibodies were rabbit anti-RPL26 (Abcam) and rabbit anti-tubulin (Cell Signaling Technology). HRP-conjugated goat anti-rabbit secondary antibody was from Jackson ImmunoResearch Laboratories. SILAC amino acids were purchased from Cambridge Isotopes Laboratories. All other reagents were from Sigma Aldrich unless otherwise specified.

Cell culture and synchronization

HeLa S3 cells were grown in DMEM (Invitrogen) supplemented with 10% fetal calf serum, 2 mM L-glutamine, and 100 U/mL penicillin/streptomycin (Biological Industries). For double-thymidine block, cells were treated with 2 mM thymidine for 19 h, released from G1/S block in fresh DMEM for 9 h, treated again with 2 mM thymidine for 18 h, released in fresh DMEM, and harvested at different time points, as indicated. Cell cycle distribution was assessed by flow cytometry using the BD Biosciences FACSort instrument after staining with propidium iodide (Sigma).

Ribosome pelleting from cultured cells

For each sample, 3.5×10^7 HeLa cells were washed once, harvested in PBS (Gibco), centrifuged at 1000*g* for 5 min at 4°C, and then frozen at −80°C for subsequent use. To purify ribosomes, cells were thawed on ice and lysed for 20 min in 500 µL of polysome buffer (18 mM Tris at pH 7.5, 50 mM KCl, 10 mM MgCl, 10 mM NaF, 10 mM α-glycerolphosphate, 1.4 µg/mL pepstatin, 2 µg/mL leupeptin, Complete EDTA-free protease inhibitor cocktail [Roche], 1.25 mM dithiothreitol, 40 U RNase inhibitor [Invitrogen]) supplemented with Triton X-100 and deoxycholate to a final concentration of 1% each. Following centrifugation at 14,000 rpm for 10 min at 4°C, the supernatant was removed and layered on 500 µL of 2 M sucrose in polysome buffer. The sucrose cushion was centrifuged at 37,000 rpm for 4 h at 4°C in a Beckman Coulter TLA120.2 rotor, and the ribosome pellet was resuspended in 100 µL of polysome buffer and processed directly for puromycylation.

Ribosome pelleting from mouse brain tissues

Ribosomes were extracted from mouse brain tissues essentially as described in Darnell et al. (2011), with some modifications. Briefly, 3-wk-old C57BL mice were sacrificed by isoflurane anesthesia and decapitation. Brains were removed and flash-frozen in liquid nitrogen. Prior to PUNCH-P analysis, brains were homogenized in 1 mL of polyribosome buffer with 10 strokes in a dounce homogenizer. NP-40 was added to a final concentration of 1% and incubated for 10 min on ice. The homogenate was spun at 2000*g* for 10 min at 4°C. The supernatant was respun at 20,000*g* for 10 min at 4°C, and the resulting supernatant was layered on 500 µL of 2 M sucrose in polysome buffer. The sucrose cushion was centrifuged at 37,000 rpm for 4 h at 4°C in a Beckman Coulter TLA120.2 rotor, and the ribosome pellet was resuspended in 100 µL of polysome buffer and processed directly for puromycylation.

Puromycylation and streptavidin capture

Resuspended ribosomes were incubated for the indicated times at 37°C either with or without Biot-PU at a ratio of 100 pmol per 1 OD_{254} ribosomes. The reaction was terminated by the addition of Laemmli sample buffer for direct Western blotting or high-stringency wash buffer (100 mM Tris HCl at pH 7.5, 2% SDS, 8 M urea, 150 mM NaCl) for streptavidin capture. The mix was tumbled overnight at room temperature with 50 µL of streptavidin agarose slurry. The beads were then washed four times with 1 mL of high-stringency buffer followed by one 30-min wash in the same buffer at room temperature and then washed for 30 min in 1 mL of high-salt buffer (100 mM Tris HCl at pH 7.5, 1 M NaCl) and five times with ultrapure water. The beads were then incubated for 30 min in 1 mM DTT and then 50 mM iodoacetamide (in the dark) and washed twice with 50 mM ammonium bicarbonate. For MS analysis, beads were resuspended in 50 mM ammonium bicarbonate, and proteins were digested overnight with 0.4 µg of sequencing-grade trypsin (Promega). After overnight incubation, digests were acidified with 0.1% TFA and purified on C_{18} StageTips (Rappsilber et al. 2007). For Western blot analysis, proteins were released from washed streptavidin beads by boiling in elution buffer (2% SDS, 3 mM biotin, 8 M urea in PBS) for 30 min at 96°C, as previously described (Rybak et al. 2004).

Western blot analysis of puromycylated peptides

For detection of puromycylated peptides, samples were resolved on a 10% or 12% SDS-PAGE and transferred to a nitrocellulose membrane. The membrane was stained with ponceau S, photographed, and blocked for 1 h with 4% BSA in TBST followed by incubation for 1 h with 1:500 streptavidin-HRP in TBST at room temperature or overnight with 1:10,000 anti-puromycin antibody in 4% BSA in TBST. The membrane was washed three times in TBST for 5 min each, and detection was performed using standard ECL technique (GE Healthcare).

Polysome profile analysis

Polysome profile analysis was performed as described previously (Sivan et al. 2007). Briefly, ribosomes were pelleted, labeled with Biot-PU, layered on a 10%–50% linear sucrose gradient in polysome buffer, centrifuged at 37,000 rpm for 100 min at 4°C in an SW41 Beckman Coulter rotor; and fractionated with absorption measured continuously at 254 nm using a Teledyne ISCO UA-6 UV/VIS detector. Fractions were collected and subjected to Western blot analysis as described above.

pSILAC

For pSILAC experiments, cells were cultured in medium deprived of the natural amino acids lysine and arginine and supplemented with light (Lys0 and Arg0), medium (Lys4 and Arg6), or heavy (Lys8 and Arg10) versions of these amino acids. Instead of standard fetal bovine serum, culture medium was supplemented with dialyzed serum. Cells were first cultured in light medium and then pulse-labeled with medium-heavy or heavy medium for 2 h or 10 h. Parallel labeling with medium and heavy medium served as a biological replicate in the same MS run. Each treatment was also conducted in independent duplicates.

Protein digestion LC-MS/MS analysis

PUNCH-P and pSILAC samples were analyzed using single 4-h runs (including loading, gradient, and wash duration) and in replicates as indicated for each experiment. LC-MS/MS analysis was performed on an EASY-nLC1000 ultrahigh-performance LC (UHPLC) (Thermo Scientific) coupled on line to the Q-Exactive mass spectrometer (Thermo Scientific). Peptides were separated on a 50-cm column with 2-µm pepmap beads (Dionex) and connected to the MS through an EASY-spray ionization source. Peptides were loaded onto the column in buffer A (0.5% acetic acid) and separated with a 200-min gradient of 5%–30% buffer B (80% acetonitrile, 0.5% acetic acid) followed by a 10-min wash with 95% buffer B. MS analysis was performed using a data-dependent top 10 method. MS spectra were acquired at 70,000 resolution (at 200 Th) with a target value of 10^6 ions. MS/MS spectra were acquired at 17,500 resolution with a target value of 10^5 ions. Dynamic exclusion option was enabled, with exclusion duration of 20 sec.

Data analysis

Raw MS files were analyzed with MaxQuant software (Cox and Mann 2008) and the Andromeda search engine (Cox et al. 2011). MS/MS were searched against the UniProt human database and an additional list of common contaminants, including avidin. Data were filtered with a 1% FDR on the peptide level and the protein level. The "match between runs" option was enabled to transfer identification between runs based on their accurate mass and retention time. Protein abundance was determined as the summed peptide intensities. Bioinformatic analysis was performed using the Perseus program in the MaxQuant environment. *t*-tests and ANOVA were performed with 5% FDR and S0 = 0.5 (Tusher et al. 2001). Prior to the *t*-test, data were filtered to have a minimum of two values in at least one of the triplicate noncontrol samples. The missing values were then replaced by a constant value (around the lowest-intensity value). Hierarchical clustering of proteins was performed on logarithmized intensities after *Z*-score normalization of the data using Euclidean distances.

RNA preparation and qPCR

Equal-volume fractions of sucrose gradients were collected into SDS at a final concentration of 1%. The samples were incubated with 100 µg of proteinase K for 30 min at 37°C, and RNA was extracted with an equal volume of phenol:chloroform:isoamyl (Sigma) followed by centrifugation at 12,000*g* for 15 min. The aqueous phase was precipitated with 1 vol of isopropanol. Following overnight incubation at −20°C, RNA was pelleted at 12,000*g* for 30 min at 4°C, washed twice with ice-cold 75% ethanol, and resuspended in water. cDNA was prepared with equal amounts of RNA from each fraction using poly-dT and Verso cDNA enzyme according to the manufacturer's instructions. cDNAs were amplified by qPCR using QuantaBio Fast SYBR mix with 1 µM primers (sequences included below). qPCR was performed using Step-One (Life Technologies) RT–PCR protocol with 60°C as annealing temperature. Relative *CALR* mRNA amounts were calculated as $RQ = 2^{\Delta Ct}$, where ΔCt is the Ct of *CALR* in fraction × −Ct of *CALR* in fraction 1. Relative RNA amounts for other mRNAs were calculated as $RQ = 2^{-\Delta\Delta Ct}$, where ΔΔCt is ΔCt for a specific mRNA in fraction × −ΔCt for *CALR* in the same fraction. Error bars refer to technical replicates of qPCR measurements within single experiments.

qPCR primer pairs

qPCR primer pairs were as follows: BRIP1 NM_032043 (F: GC TATTGGGCGCTGGGAGTCG; R: GCAACGCTCTGAGCTC CGATT), CALR NM_004343 (F: ATCATGTTTGGTCCCG ACATC; R: TCATCCTTGCAACGGATGTC), CCNB1 NM_ 031966 (F: AGCTGCTGCCTGGTGAAGAG; R: GCCATGTTG

ATCTTCGCCTTA), CCRN4L NM_012118 (F: CGATTCAAGC TAGTCAACAGTGC; R: CTTTTAGATGGGTAACAGCGATGC), CYCS NM_018947 (F: ACCTTCCATCTTGGCTAGTTGTG; R: ATCGCTTGAGCCTGGGAAATAG), FOSL1 NM_005438 (F: AT TTCCCATTTGTGCCAGAG; R: CAGGAAGAGGGTGATGG AGA), GPSM2 NM_013296 (F: CCAAAGGGAAAAGTTTTG GT; R: CTGAAGTTGCCAAGGAGGTA), and PCF11 NM_015885 (F: GAAGATCAAGATGTTCCAGATC; R: GTTCTTCCAGAT CAGCTATCTC).

Acknowledgments

O.E.S. acknowledges support from the Israel Science Foundation (grants 131/07 and 1036/12). T.G. is supported by funds from Tel Aviv University.

References

Blobel G, Sabatini D. 1971. Dissociation of mammalian polyribosomes into subunits by puromycin. *Proc Natl Acad Sci* **68:** 390–394.

Calkhoven CF, Muller C, Leutz A. 2002. Translational control of gene expression and disease. *Trends Mol Med* **8:** 577–583.

Clark IE, Wyckoff D, Gavis ER. 2000. Synthesis of the posterior determinant Nanos is spatially restricted by a novel cotranslational regulatory mechanism. *Curr Biol* **10:** 1311–1314.

Cox J, Mann M. 2008. MaxQuant enables high peptide identification rates, individualized p.p.b.-range mass accuracies and proteome-wide protein quantification. *Nat Biotechnol* **26:** 1367–1372.

Cox J, Neuhauser N, Michalski A, Scheltema RA, Olsen JV, Mann M. 2011. Andromeda: A peptide search engine integrated into the MaxQuant environment. *J Proteome Res* **10:** 1794–1805.

Darnell JC, Van Driesche SJ, Zhang C, Hung KY, Mele A, Fraser CE, Stone EF, Chen C, Fak JJ, Chi SW, et al. 2011. FMRP stalls ribosomal translocation on mRNAs linked to synaptic function and autism. *Cell* **146:** 247–261.

David A, Dolan BP, Hickman HD, Knowlton JJ, Clavarino G, Pierre P, Bennink JR, Yewdell JW. 2012. Nuclear translation visualized by ribosome-bound nascent chain puromycylation. *J Cell Biol* **197:** 45–57.

de Boer E, Rodriguez P, Bonte E, Krijgsveld J, Katsantoni E, Heck A, Grosveld F, Strouboulis J. 2003. Efficient biotinylation and single-step purification of tagged transcription factors in mammalian cells and transgenic mice. *Proc Natl Acad Sci* **100:** 7480–7485.

Dieterich DC, Link AJ, Graumann J, Tirrell DA, Schuman EM. 2006. Selective identification of newly synthesized proteins in mammalian cells using bioorthogonal noncanonical amino acid tagging (BONCAT). *Proc Natl Acad Sci* **103:** 9482–9487.

Eichelbaum K, Winter M, Diaz MB, Herzig S, Krijgsveld J. 2012. Selective enrichment of newly synthesized proteins for quantitative secretome analysis. *Nat Biotechnol* **30:** 984–990.

Fan F, Jin S, Amundson SA, Tong T, Fan W, Zhao H, Zhu X, Mazzacurati L, Li X, Petrik KL, et al. 2002. ATF3 induction following DNA damage is regulated by distinct signaling pathways and over-expression of ATF3 protein suppresses cells growth. *Oncogene* **21:** 7488–7496.

Garbarino-Pico E, Green CB. 2007. Posttranscriptional regulation of mammalian circadian clock output. *Cold Spring Harb Symp Quant Biol* **72:** 145–156.

Groisman I, Huang YS, Mendez R, Cao Q, Theurkauf W, Richter JD. 2000. CPEB, maskin, and cyclin B1 mRNA at the mitotic apparatus: Implications for local translational control of cell division. *Cell* **103:** 435–447.

Guo H, Ingolia NT, Weissman JS, Bartel DP. 2010. Mammalian microRNAs predominantly act to decrease target mRNA levels. *Nature* **466:** 835–840.

Hobden AN, Cundliffe E. 1978. The mode of action of α sarcin and a novel assay of the puromycin reaction. *Biochem J* **170:** 57–61.

Holcik M, Sonenberg N. 2005. Translational control in stress and apoptosis. *Nat Rev Mol Cell Biol* **6:** 318–327.

Howden AJ, Geoghegan V, Katsch K, Efstathiou G, Bhushan B, Boutureira O, Thomas B, Trudgian DC, Kessler BM, Dieterich DC, et al. 2013. QuaNCAT: Quantitating proteome dynamics in primary cells. *Nat Methods* **10:** 343–346.

Huszar D, Theoclitou ME, Skolnik J, Herbst R. 2009. Kinesin motor proteins as targets for cancer therapy. *Cancer Metastasis Rev* **28:** 197–208.

Ingolia NT, Ghaemmaghami S, Newman JR, Weissman JS. 2009. Genome-wide analysis in vivo of translation with nucleotide resolution using ribosome profiling. *Science* **324:** 218–223.

Joyce D, Albanese C, Steer J, Fu M, Bouzahzah B, Pestell RG. 2001. NF-κB and cell-cycle regulation: The cyclin connection. *Cytokine Growth Factor Rev* **12:** 73–90.

Kiick KL, Saxon E, Tirrell DA, Bertozzi CR. 2002. Incorporation of azides into recombinant proteins for chemoselective modification by the Staudinger ligation. *Proc Natl Acad Sci* **99:** 19–24.

Kim ST, Xu B, Kastan MB. 2002. Involvement of the cohesin protein, Smc1, in Atm-dependent and independent responses to DNA damage. *Genes Dev* **16:** 560–570.

Kramer G, Sprenger RR, Back J, Dekker HL, Nessen MA, van Maarseveen JH, de Koning LJ, Hellingwerf KJ, de Jong L, de Koster CG. 2009. Identification and quantitation of newly synthesized proteins in *Escherichia coli* by enrichment of azidohomoalanine-labeled peptides with diagonal chromatography. *Mol Cell Proteomics* **8:** 1599–1611.

Lee S, Liu B, Huang SX, Shen B, Qian SB. 2012. Global mapping of translation initiation sites in mammalian cells at single-nucleotide resolution. *Proc Natl Acad Sci* **109:** E2424–E2432.

Liang YC, Hsu CY, Yao YL, Yang WM. 2013. PARP-2 regulates cell cycle-related genes through histone deacetylation and methylation independently of poly(ADP-ribosyl)ation. *Biochem Biophys Res Commun* **431:** 58–64.

Lindqvist A, Rodriguez-Bravo V, Medema RH. 2009. The decision to enter mitosis: Feedback and redundancy in the mitotic entry network. *J Cell Biol* **185:** 193–202.

Liu J, Xu Y, Stoleru D, Salic A. 2012. Imaging protein synthesis in cells and tissues with an alkyne analog of puromycin. *Proc Natl Acad Sci* **109:** 413–418.

Losada A, Hirano T. 2005. Dynamic molecular linkers of the genome: The first decade of SMC proteins. *Genes Dev* **19:** 1269–1287.

Marzluff WF, Duronio RJ. 2002. Histone mRNA expression: Multiple levels of cell cycle regulation and important developmental consequences. *Curr Opin Cell Biol* **14:** 692–699.

Miki H, Setou M, Kaneshiro K, Hirokawa N. 2001. All kinesin superfamily protein, KIF, genes in mouse and human. *Proc Natl Acad Sci* **98:** 7004–7011.

Mumberg D, Wick M, Burger C, Haas K, Funk M, Muller R. 1997. Cyclin ET, a new splice variant of human cyclin E with a unique expression pattern during cell cycle progression and differentiation. *Nucleic Acids Res* **25:** 2098–2105.

Nagaraj N, Wisniewski JR, Geiger T, Cox J, Kircher M, Kelso J, Paabo S, Mann M. 2011. Deep proteome and transcriptome mapping of a human cancer cell line. *Mol Syst Biol* **7:** 548.

Nottrott S, Simard MJ, Richter JD. 2006. Human let-7a miRNA blocks protein production on actively translating polyribosomes. *Nat Struct Mol Biol* **13:** 1108–1114.

Pestka S. 1971. Inhibitors of ribosome functions. *Annu Rev Microbiol* **25:** 487–562.

Petersen CP, Bordeleau ME, Pelletier J, Sharp PA. 2006. Short RNAs repress translation after initiation in mammalian cells. *Mol Cell* **21:** 533–542.

Pines J, Hunter T. 1989. Isolation of a human cyclin cDNA: Evidence for cyclin mRNA and protein regulation in the cell cycle and for interaction with p34cdc2. *Cell* **58:** 833–846.

Rao PN, Engelberg J. 1968. Mitotic duration and its variability in relation to temperature in HeLa cells. *Exp Cell Res* **52:** 198–208.

Rappsilber J, Mann M, Ishihama Y. 2007. Protocol for micro-purification, enrichment, pre-fractionation and storage of peptides for proteomics using StageTips. *Nat Protoc* **2:** 1896–1906.

Riabowol K, Schiff J, Gilman MZ. 1992. Transcription factor AP-1 activity is required for initiation of DNA synthesis and is lost during cellular aging. *Proc Natl Acad Sci* **89:** 157–161.

Robinson BH, Oei J, Saunders M, Gravel R. 1983. [3H]biotin-labeled proteins in cultured human skin fibroblasts from patients with pyruvate carboxylase deficiency. *J Biol Chem* **258:** 6660–6664.

Rybak JN, Scheurer SB, Neri D, Elia G. 2004. Purification of biotinylated proteins on streptavidin resin: A protocol for quantitative elution. *Proteomics* **4:** 2296–2299.

Schmidt EK, Clavarino G, Ceppi M, Pierre P. 2009. SUnSET, a nonradioactive method to monitor protein synthesis. *Nat Methods* **6:** 275–277.

Schwanhausser B, Gossen M, Dittmar G, Selbach M. 2009. Global analysis of cellular protein translation by pulsed SILAC. *Proteomics* **9:** 205–209.

Schwanhausser B, Busse D, Li N, Dittmar G, Schuchhardt J, Wolf J, Chen W, Selbach M. 2011. Global quantification of mammalian gene expression control. *Nature* **473:** 337–342.

Sigoillot FD, Huckins JF, Li F, Zhou X, Wong ST, King RW. 2011. A time-series method for automated measurement of changes in mitotic and interphase duration from time-lapse movies. *PLoS ONE* **6:** e25511.

Sivan G, Kedersha N, Elroy-Stein O. 2007. Ribosomal slowdown mediates translational arrest during cellular division. *Mol Cell Biol* **27:** 6639–6646.

Sivan G, Aviner R, Elroy-Stein O. 2011. Mitotic modulation of translation elongation factor 1 leads to hindered tRNA delivery to ribosomes. *J Biol Chem* **286:** 27927–27935.

Starck SR, Green HM, Alberola-Ila J, Roberts RW. 2004. A general approach to detect protein expression in vivo using fluorescent puromycin conjugates. *Chem Biol* **11:** 999–1008.

Sugiyama T, Sugioka-Sugiyama R, Hada K, Niwa R. 2012. Rhn1, a nuclear protein, is required for suppression of meiotic mRNAs in mitotically dividing fission yeast. *PLoS ONE* **7:** e42962.

Tagwerker C, Flick K, Cui M, Guerrero C, Dou Y, Auer B, Baldi P, Huang L, Kaiser P. 2006. A tandem affinity tag for two-step purification under fully denaturing conditions: Application in ubiquitin profiling and protein complex identification combined with in vivocross-linking. *Mol Cell Proteomics* **5:** 737–748.

Tusher VG, Tibshirani R, Chu G. 2001. Significance analysis of microarrays applied to the ionizing radiation response. *Proc Natl Acad Sci* **98:** 5116–5121.

Vaughan MH Jr, Pawlowski PJ, Forchhammer J. 1971. Regulation of protein synthesis initiation in HeLa cells deprived of single essential amino acids. *Proc Natl Acad Sci* **68:** 2057–2061.

Vogel C, Marcotte EM. 2012. Insights into the regulation of protein abundance from proteomic and transcriptomic analyses. *Nat Rev Genet* **13:** 227–232.

Whitfield ML, Zheng LX, Baldwin A, Ohta T, Hurt MM, Marzluff WF. 2000. Stem-loop binding protein, the protein that binds the 3′ end of histone mRNA, is cell cycle regulated by both translational and posttranslational mechanisms. *Mol Cell Biol* **20:** 4188–4198.

Yasumi M, Sakisaka T, Hoshino T, Kimura T, Sakamoto Y, Yamanaka T, Ohno S, Takai Y. 2005. Direct binding of Lgl2 to LGN during mitosis and its requirement for normal cell division. *J Biol Chem* **280:** 6761–6765.

Novel proteomic approach (PUNCH-P) reveals cell cycle-specific fluctuations in mRNA translation

Ranen Aviner, Tamar Geiger and Orna Elroy-Stein

Genes Dev. 2013, **27:** originally published online August 9, 2013
Access the most recent version at doi:10.1101/gad.219105.113